01 Apr 2023

Efficient Recycling of Waste Rubber in a Sustainable Fiber-Reinforced Mortar and its Damping and Energy Dissipation Capacity

Haodao Li

Wu Jian Long

Kamal Khayat
Missouri University of Science and Technology, khayatk@mst.edu

Recommended Citation

H. Li et al., "Efficient Recycling of Waste Rubber in a Sustainable Fiber-Reinforced Mortar and its Damping and Energy Dissipation Capacity," *Cement and Concrete Composites*, vol. 138, article no. 104963, Elsevier, Apr 2023.
The definitive version is available at https://doi.org/10.1016/j.cemconcomp.2023.104963

Cement and Concrete Composites 138 (2023) 104963

Contents lists available at ScienceDirect

Cement and Concrete Composites

journal homepage: www.elsevier.com/locate/cemconcomp

Efficient recycling of waste rubber in a sustainable fiber-reinforced mortar and its damping and energy dissipation capacity

Haodao Li [a,b], Wu-Jian Long [b], Kamal H. Khayat [a,*]

[a] Department of Civil, Architectural and Environmental Engineering, Missouri University of Science and Technology, Rolla, MO, 65401, USA
[b] Key Lab of Coastal Urban Resilient Infrastructure, MOE, Guangdong Provincial Key Laboratory of Durability for Marine Civil Engineering, College of Civil and Transportation Engineering, Shenzhen University, Shenzhen, 518060, Guangdong, PR China

ARTICLE INFO

Keywords:
High-volume fly ash
Low-temperature plasma treatment
Material damping characteristic
Polyvinyl alcohol fiber
Waste crumb rubber

ABSTRACT

A great number of waste tires are discarded in landfills, occupying land resources, and severely endangering the ecosystem. Upcycling these wastes as aggregates to partially substitute natural sand and develop structure-function integration in concrete structures is a desirable solution. In this study, a sustainable fiber-reinforced rubberized mortar with superior material damping and moderate strength is developed by combined use of waste crumb rubber (WCR) incorporated at 0, 30%, and 60%, by volume of sand, and polyvinyl alcohol (PVA) fiber added at 0, 0.5%, and 1%, by volume, in a high-volume fly ash binder system. Low-temperature plasma (LTP) pre-treatment of the WCR was applied to compensate for strength loss resulting from the incorporation of a large portion of the WCR, which increases the recycling efficiency of the WCR. The macro tests of static and dynamic mechanical properties were used to characterize the material damping and energy dissipation capacity, followed by microstructural tests to evaluate the enhanced damping mechanisms. Test results show that the combination of 60% LTP pre-treated WCR and 1% PVA fiber can secure the highest damping capacity and energy dissipation ratio without a significant strength drop. The use of discarded WCR is therefore promising to substitute conventional sand and design functionalized intrinsic viscoelastic cement composites that can be adopted in anti-vibrational technology applications.

1. Introduction

With the accelerated growth of industrialization and urbanization, the large amount of industrial discarded waste has dramatically increased. Such waste stream materials contain potential ecological threats, such as toxicity, radioactivity, and combustibility. According to recently published statistics on solid waste pollution [1], the stock of global solid waste reached 38 billion tons, of which China was as high as 7 billion tons in 2020. Finding solutions to use some of these massive amounts of hazardous wastes in construction materials or other industrial applications can offset natural and non-renewable resources and alleviate pressure on landfills. In China, the 7 billion tons of solid waste can take up nearly 21 million acres of the landfill to store. It is worth noting that the current industrial waste of discarded tires is growing at an annual rate of 100 million tons globally, and yet they account for 40% of solid waste output that is not currently unused [2]. Meanwhile, the uncontrolled growth of waste tires has generated problems concerning waste management. These tires are complex and contain synthetic rubbers, carbon black, metallic fibers, and organic residues [3]. Traditional waste recycling methods include landfill and incineration after the end of their serviceable life; however, it not only causes extreme environmental pollution but can even endanger human health. Therefore, in order to reduce the waste of land resources, the rapid and efficient recycling of such obsolete tires has undoubtedly become an urgent challenge.

It is widely accepted that crumb rubber can be considered as an alternative coarse/fine aggregate, which can be obtained from discarded tires under a series of physical treatments (e.g., crushing, crumbling, separating, grinding, and washing). This aims to tackle an extreme shortage of natural resources and meet the imminent need for waste up-recycling. Waste crumb rubber (WCR) aggregate is regarded as a viscoelastic material with good elastic deformation, which contributes to decreasing the unit weight, enhancing electrical resistance and thermal insulation, greatly improving ductility and toughness, and strengthening intrinsic resistance to the vibrational deterioration in concrete [4–7]. These improved characteristics, especially for superior ductility and

* Corresponding author.
E-mail address: kkhayat@mst.edu (K.H. Khayat).

https://doi.org/10.1016/j.cemconcomp.2023.104963
Received 12 June 2022; Received in revised form 24 December 2022; Accepted 28 January 2023
Available online 7 February 2023

energy dissipation capacity, facilitate rubber concrete turning into a promising material for bridge piers, highway pavements, public squares, railway barriers, and other infrastructure applications [8,9]. Mei et al. [10] used 0.075–2 mm fine rubber particles as the aggregate substitution in recycled rubber concrete and studied its failure performance. It stated that concrete specimens incorporating rubber can withstand measurable post-failure compression load and significant displacement, and their deformations will be partially recoverable. This improved ductile mode and toughness behavior of rubberized concrete were also reported by Aliabdo et al. [11] and it concluded that at a 15% substitute of fine aggregate, the modulus of toughness for waste rubber concrete is 15% higher than that of control concrete. Lin et al. [12] reported a substantial increase in the concrete damping ratio of rubberized concrete with the increase of rubber content and suggested that 2.5 vol% was the optimum substitution of waste rubber in the application where the damping capacity of concrete is required, such as railway stations.

However, a critical technical challenge that hinders the re-use of waste rubber is the significant reduction in mechanical properties, most notably in compressive strength, which is mainly attributed to the weak bond between the rubber particles and the cement matrix [13,14]. And also, the hydrophobic nature of the rubber can block the movement of water in the mixture hence retarding cement hydration [15]. Several researchers reported a significant reduction of 10%–80% in compressive and flexural strengths of rubberized concrete with an increasing quantity of waste rubber content [8,16,17]. Limiting the total fine aggregate replacement to 30%, by volume, seems to have a confined effect on the compressive strength of waste rubberized concrete. Additionally, the larger nominal maximum particle size and gap gradation of WCR lead to the worse mechanical properties of rubberized concrete [18]. An optimized replacement ratio and particle size distribution of rubber aggregate to balance the properties of rubberized concrete is essential to promote the high recycling efficiency of WCR. Beneficially, the inferior deficiencies associated with WCR can be effectively mitigated based on the pre-treatments, such as water or alkaline hydroxide soaking, oxidation, microwave processing, admixture and chemical coating, and thermal treatment [19–22]. In addition, another novel technique treated by low-temperature plasma (LTP) can be used to modify the hydrophobic surface of rubber particles [23]. Cheng et al. [24] investigated the effect of plasma polymerization of ethanol on the contact angle between crumb rubber and water and concluded that a significant reduction from 122° to 36° after surface treatment for 1 h. Nisticò et al. [25] found compressive strength, flexural strength, and toughness of rubber concrete can be improved using plasma modification for WCR and concluded that the plasma treatment can effectively enhance both intrinsic adhesion and roughness of the rubber-matrix interface and thus the overall concrete strength and toughness.

To further optimize the substitute rate of WCR aggregate and outdo its visco-elastic nature as anti-vibration functionalized, additional fiber-reinforced technology is reasonably preferred due to the excellent improvements of fibers. As one of the most popular fiber types commonly used in concrete, polyvinyl alcohol (PVA) fiber has a high elastic modulus, high tensile strength, adequate bond to the cement matrix, and excellent chemical resistance [26]. These outstanding characteristics of PVA fiber mainly contribute to the tensile properties of concrete and the bridging effect of PVA fiber for voids or micro-cracks can make up for the low flexural behavior of cement matrix [27,28]. Additionally, with the addition of PVA fiber, the energy dissipating and damping performance of composites can be significantly improved by the microplastic strain of fractured fibers and relative friction between fiber-matrix interfaces under dynamic loads [29]. Therefore, the possibility of incorporating PVA fibers into mortar made with WCR as fine aggregate to compensate for the mechanical defects resulting from WCR and further improve vibrational resistance will be investigated in this study. Previous studies have reported that discarded waste rubber can be feasibly tolerated in PVA fiber-reinforced composites (PVA-FRC). Wang et al. [30] introduced fiber-reinforced rubber concrete made with 0.5% PVA fiber and different replacement ratios of rubber aggregate (15%, 20%, and 25%) and concluded that the post-cracking extension and fracture energy can be largely improved due to fiber crack bridging. Chen et al. [31] developed impact-resistant engineered cementitious composites (ECC) using waste crumb rubber (up to 40% by volume) and PVA fibers. It was concluded that the rubberized ECC has higher energy dissipation capacity than normal ECC, especially under cold temperatures, even though significantly sacrifices compressive strength. This innovative rubberized ECC with high ductility using a combination of waste rubber and PVA fibers was also successfully developed by AI-Fakih et al. [32]. Ma et al. [33] studied the potential use of rubber powder obtained by cutting waste tires in PVA-FRC and reported that the rubber powder was beneficial to improve the damping ratio of PVA-FRC, but it aggravated its interface defects, indicating 5 vol% and PVA fiber was the most optimal mixing proportion to balance the strength and damping performance. However, these current studies did not address the considerable loss of compressive strength brought by incorporating WCR, and material damping and energy dissipation capacity were not fully characterized.

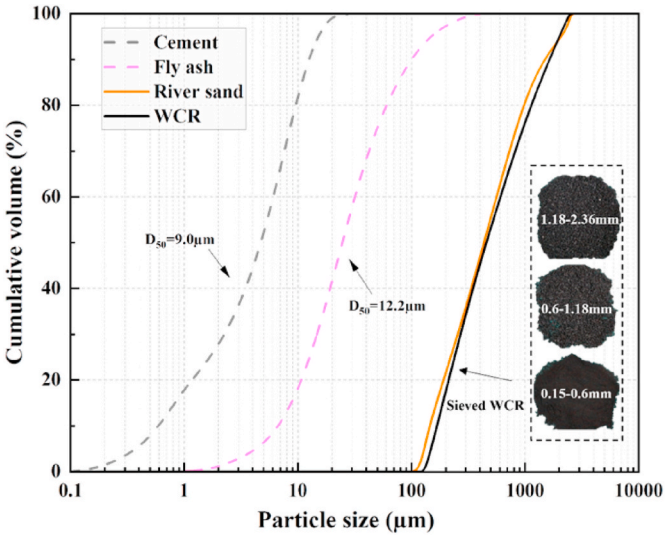

Fig. 1. Particle-size distributions of binder materials and fine aggregates.

In this study, the potential feasibility of using WCR and PVA fiber in mortar mixtures, and its mechanical and damping properties are thoroughly investigated. LTP surface treatment for WCR aggregate was innovatively adopted to weaken its surface defects and provide a solution for the compressive strength loss that comes with using WCR, increasing the substitution rate of the WCR and maximizing its recycling efficiency. A high-volume fly ash (HVFA) binder system was selected for the fiber-reinforced mortar (FRM) and the PVA fiber-reinforced rubberized mortar (PVA-FRRM) systems. This contributes to reducing the cement content and effectively improve fracture toughness and ductility of the PVA-FRC [34]. In addition, the material damping and energy dissipation capacity of FRM and PVA-FRRM were characterized by a competent non-destructive device, and their pore structures and micromorphology were further microscopically characterized to explain the improved damping mechanism. Ultimately, the novel PVA-FRRM system can be developed to exhibit moderate mechanical strength and excellent material damping characteristics for use in non-structural and anti-vibrational applications.

2. Materials and methods

2.1. Materials

A Type 42.5 R ordinary Portland cement (OPC) and a Class F fly ash

Table 1
Physical characteristics of fine aggregates used in this study.

	River sand	Waste crumb rubber
Roughness	0.5	0.6
Apparent density (g/cm^3)	2.63	1.22
Bulky density (g/cm^3)	1.49	0.57
Water absorption (%)	0.55	0.65
Shear modulus (MPa)	1	2.9×10^4
Homogeneity	1.62	1.07

(FA) were used. The specific surface areas of the OPC and FA are 371 and 362 m^2/kg, respectively, and their specific gravities are 3.00 and 2.33, respectively. The WCR particles were acquired from a tire-recycling company. The WCR was mechanically shredded, crushed, ground, and washed. To further minimize or even eliminate the negative effect caused by aggregate size variations of the crumbled rubber, the WCR particles were sieved through a vibrating screen to secure essentially a similar particle size distribution (PSD) of river sand used for mortar. The PSD curves of the binders and fine aggregates, determined by a laser particle size analyzer, are shown in Fig. 1. The comparison of the physical properties between the river sand and WCR is shown in Table 1. The WCR has a higher shear modulus compared to the river sand, which is a key characteristic needed to improve the damping characteristics. The microstructural morphology of WCR particles is shown in Fig. 2 and there are many fine pores ranging among the micron level on the surface.

The REC-15 × 12 type of PVA fiber with a diameter of 40 μm and a length of 12 mm was selected for this study. The fiber shows excellent mechanical properties including a tensile strength of 1560 MPa, a tensile strain of 6.5%, and a tensile modulus of 41 GPa.

2.2. Mixture design of PVA-FRRMs

Seven mortar mixtures including reference group, FRMs, and PVA-FRRMs were developed with the constant ratio of water-to-binder (w/b) of 0.40. The detailed proportions of the corresponding mixtures are summarized in Table 2. A fixed FA-to-cement ratio of 1.22 was adopted in the HVFA system prepared with 55% substitution of FA by volume of total binder. Substantially replacing cement with FA contributes to alleviating the strong cohesion between the fiber and cement matrix and also reducing carbon dioxide (CO_2) emissions induced by cement manufacturing which can further achieve environmentally beneficial mixtures [34]. Given that the WCR has a lower density than the river sand, treated WCR particles were partially incorporated at 30% and 60% substitution rates, by volume of sand, to achieve favorable functionalization in the anti-vibration application field. Oil-treated PVA fibers were also mixed at relatively low content of 0.5% and 1.0%, by volume. In this study, a superplasticizer (SP) of 0.2% was used to ensure a high fluidity of the PVA-FRRM mixtures.

The detailed mixing procedures are shown in Fig. 3. Firstly, dry solid materials including cement and FA, WCR particles, and river sand were mixed for 2 min. The SP diluted with half of the mixing water was then introduced and mixed for 3 min at a normal mixing rate. The PVA fibers were then added slowly to avoid the cluster of the fibers. After 30 s, the remaining half of the mixing water was subsequently introduced into the fiber-reinforced mixture for another 4 min at a high mixing rate. The SP dosage was adjusted to secure the desired workability.

Each mixture was cast into steel molds to determine the static mechanical and material damping properties. The mortar samples were demolded after 1 d and stored in a standard curing room at 20 ± 2 °C and RH ≥ 95% for further curing.

Table 2
Mixture proportions of eco-friendly fiber-reinforced mortars.

Mix ID	Ingredient (kg/m^3)						
	Cement	FA	River sand	WCR	Water	SP	PVA fiber (vol. %)
Reference	408	499	907	0	363	1.81	0
RP0.5			907	0			0.5
RP1.0			907	0			1
R30P0.5			634.9	126.2			0.5
R60P0.5			362.8	294.5			0.5
R30P1.0			634.9	126.2			1
R60P1.0			362.8	294.5			1

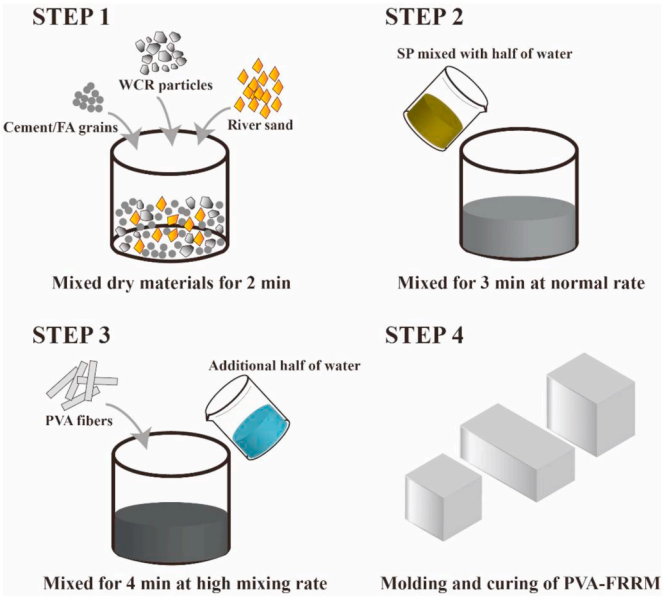

Fig. 3. Batching sequence and mixing procedure of PVA-FRRM mixtures.

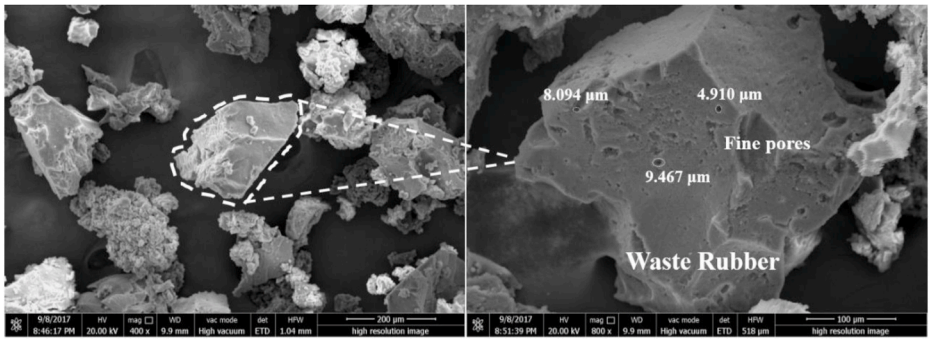

Fig. 2. Microstructural morphology of WCR particles captured by SEM.

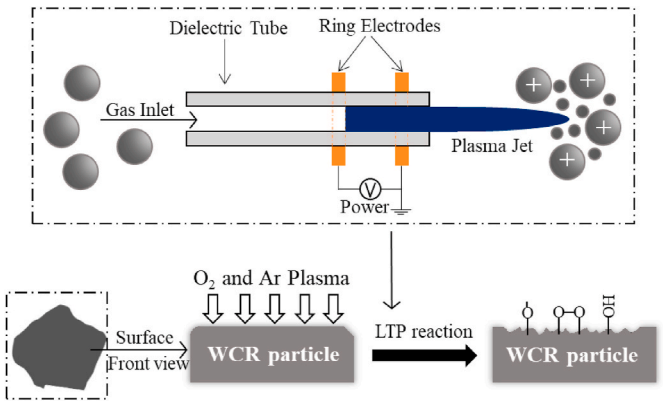

Fig. 4. Principle of O_2/Ar plasma treatment modification for the WCR particle.

2.3. Test methods

2.3.1. Low-temperature plasma treatment

The optimal replacement of WCR aggregate for rubberized concrete is approximately 20%–30%, by volume of sand; however, such a substitution rate can lead to a considerable reduction of compressive strength [19]. In this study, the low-temperature plasma (LTP) reactor (PT-DT03) was employed to pre-treat WCR particles in order to enhance surface characteristics and reduce the adverse impact on mechanical properties and improve the recycling efficiency. This treatment method can roughen the surface of the WCR aggregate and transform the hydrophobic nature of WCR particles [24]. The detailed treatment process of LTP for WCR particles is illustrated in Fig. 4. Oxygen and argon gases were selected as background gases to be injected into the reaction chamber at a flow rate of 60 sccm (standard cubic centimeter per minute), after placing and sealing the WCR particles in each batch of 1000 g. When ion beams started to bombard, the polar groups (i.e., –O, –O═O, and –OH) on the WCR surface were activated, which can reduce the surface energy and promote chemical bonding. The duration of the LTP process was 10 min for each batch under the suitable power condition of 100 W [24]. After the LTP treatment, the WCR surface became rougher, as observed in Fig. 5.

2.3.2. Contact angle test

Polarity changes of WCR particles before and after LTP pre-treatment were evaluated using the optical contact angle goniometer (OCA 15 EC). To prevent the infiltration of water into the gap between WCR particles that can result in inaccurate measurement, treated and untreated single flat strips of WCR were carefully selected. Fig. 6 illustrates the results of the contact angle test showing that the hydrophobic nature of the WCR particle was effectively improved by the LTP treatment. The treated WCR particles became more hydrophilic. As shown in Fig. 6(a), the contact angles of the untreated particle on the left and right sides were 74.4° and 75.2°, respectively. Both values are lower than 90°, which reflects a strong water repellency of the crumb rubber with the porous surface of the WCR showing water retention. After processing in the LTP reaction chamber that was full of oxygen and argon gases, the contact angles on both sides increased to 119.4° and 118.5°, respectively, as shown in Fig. 6(b). Therefore, the contact angle test effectively proves that the WCR particles gradually transformed from hydrophobic to hydrophilic after the LTP treatment, and their surface polarizations were altered significantly.

2.3.3. Fresh property tests

The mini-slump flow and density of the seven mortar samples were characterized. The slump flow was determined by the flow table measurement using a mini-cone apparatus in accordance with GB/T 2419 [35]. The upper and bottom diameters of the mini-cone measure 70 and 100 mm, respectively, and the height is 60 mm. The mini-cone was filled in two layers with each layer rodded 25 times. The spread diameters were measured in two different directions to determine the average slump flow. The density of the mortar was measured in accordance with GB/T 50,080 [36] using a cylindrical container filled in two layers with each layer rodded 25 times.

2.3.4. Static mechanical tests

The static mechanical tests were conducted to evaluate the flexural and compressive strengths of mortar mixtures in accordance with GB/T 17,671 [37]. Prismatic samples measuring 40 mm × 40 mm × 160 mm were cast. The samples were tested after 28 days of standard curing to determine the flexural and compressive strengths. The prismatic samples were tested under three-point bending with a constant loading rate of 50 N/s. The 40-mm cube samples obtained after the bending tests were designated for the compression measurement and were tested at a constant loading rate of 2.4 kN/s.

2.3.5. Material damping tests

Damping refers to an intrinsic nature of materials that reflects one of the dynamic characteristics, which can be categorized as a passive method to absorb vibration and dissipate energy [38]. It is closely related to a sort of functionalization of concrete structures towards the anti-vibration or resistance of dynamic cyclic loads. In other words,

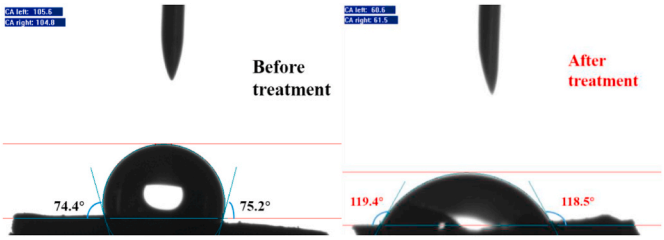

Fig. 6. Contact angle test results of WCR strips a) before and b) after LTP treatment.

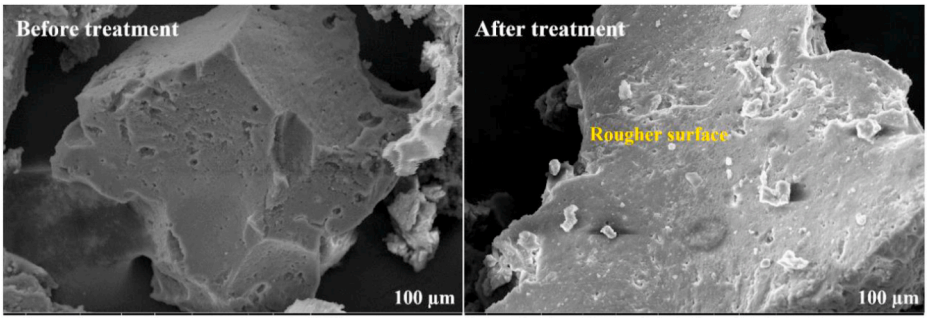

Fig. 5. Microscopic images of WCR strips before and after LTP treatment.

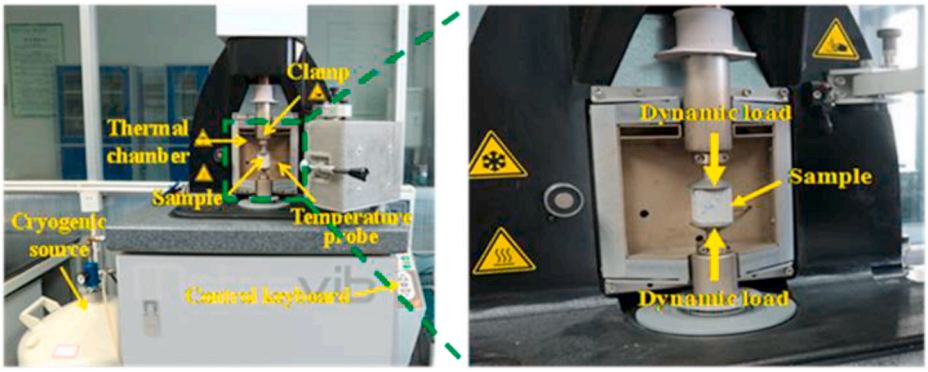

Fig. 7. Non-destructive device for dynamic mechanical analysis.

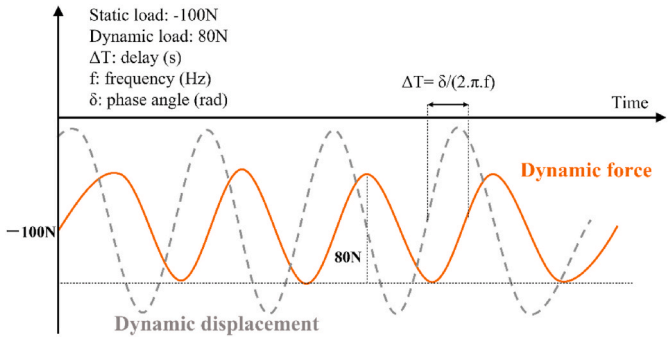

Fig. 8. Setting parameters and measurement principle of DTMA test.

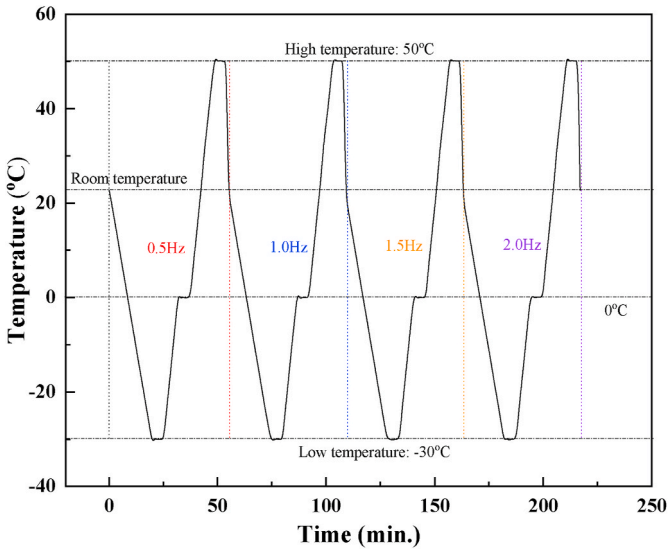

Fig. 9. Measurement protocol. Temperature profile with time collapses.

using damping concrete composites to effectively dissipate or transfer the vibrating energy instead of relying on the use of a damping device is innovative and cost-effective. Traditionally, there are three common characterization methods to evaluate the dynamic mechanical properties including the three-point dynamic bending test, split Hopkinson pressure bar (SHPB), and dynamic thermomechanical analyzer (DTMA) [39–41]. However, test samples will experience a large degree of damage in the first two tests, and strict control is needed in conducting these tests. In this study, the material damping was characterized using the third method, which is a non-destructive technique shown in Fig. 7 consisting of forced vibration oscillation to evaluate the loss modulus, storage modulus, and loss factor.

The testing principle and setting parameters are shown in Fig. 8. The basic testing principle of the DTMA apparatus is to exert a dynamic excitation of known amplitude and frequency (out of resonance) to a sample of known dimensions. For most viscoelastic materials, such as concrete composites, there is a phase shift between the dynamic force and dynamic displacement when the material is subjected to a sinusoidal vibration. In this study, the compression plate of the DTMA test was selected, and a dynamic force of 80 N and strains were initially set to yield the stiffness, dynamic modulus, and loss factor. The testing dimension of the mortar samples was 20 mm × 20 mm × 20 mm. Contact surfaces were glued between jaws on two extreme faces before testing. The static load of −100 N was also applied to fix the test sample to avoid ejection during the test and obtain accurate data. The factors affecting the damping properties of mortars in terms of testing time and vibration frequencies (0.5–2 Hz) were investigated. The effect of the desired temperature domain (−30 to 50 °C) was also evaluated to expound on the phase change of WCR aggregates under this specific freeze-high temperature span. The detailed measurement protocol of the DTMA test is illustrated in Fig. 9 and shows the excitation temperature history versus the elapsed time measured in this study. The total time range for the test was approximately 220 min for each mixture, which included the same temperature profile and time interval at each vibration frequency (0.5, 1.0, 1.5, and 2.0 Hz). At the beginning of the test, the dynamic behavior of each mixture at room temperature was recorded. As time elapsed for 20 min, there was a cooling process at a cooling rate of -3 °C/min from room temperature to −30 °C. After 3 min of holding, the temperature was increased to 0 °C for about 6 min at a heating rate of 5 °C/min and maintained at that temperature for 3 min. Subsequently, the temperature was increased to 50 °C at the same heating rate before returning to room temperature for the next measurement at a different frequency.

2.3.6. Microstructural characterization

The total porosity and pore structure and microstructural morphology of mortar mixtures were characterized using mercury intrusion porosimetry (MIP) and scanning electronic microscopy (SEM), respectively. Each group of mortars was cut into 1 mm × 1 mm × 1 mm cubic samples and immersed in acetone to stop the cement hydration reaction for the MIP and SEM tests. The maximum and minimum pressures applied with the MIP apparatus were set to 414 MPa and 345 KPa, respectively. The accelerating voltage of the SEM with the selected magnification of 1280 × 960 pixels was set to 20 kV.

3. Results and discussions

3.1. Fresh properties

The results of the mini-slump and density are summarized in Table 3.

Table 3
Fresh properties of sustainable FRMs and PVA-FRRMs.

Mix ID	Reference	RP0.5	RP1.0	R30P0.5	R60P0.5	R30P1.0	R60P1.0
Slump flow (mm)	204	196	185	177	152	167	143
Density (g/cm^3)	2.292	2.280	2.264	2.145	1.971	2.118	1.947

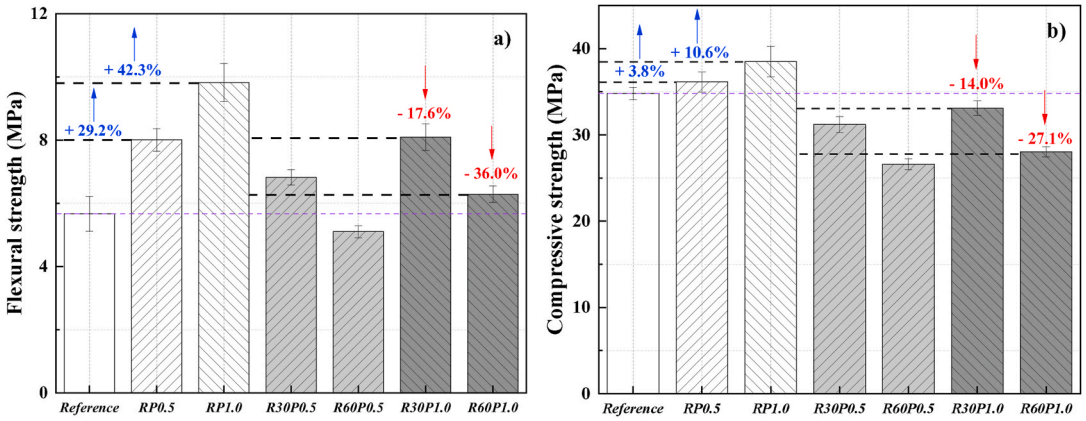

Fig. 10. Static mechanical properties of sustainable FRMs and PVA-FRRMs at the curing of 28 days. a) Flexural strength; b) Compressive strength.

In general, the mini-slump flow decreased with the addition of fiber and WCR. However, the presence of fly ash in the HVFA system contributed to increasing the mini-slump flow. The lowest value of mini-slump flow was 143 mm for the R60P1.0 mixture prepared with 60% WCR substitution and 1.0% fiber. As the fiber volume increased, the mini-slump flow decreased gradually. The mini-slump flow decreased by 4% and 9% compared to the reference mortar for mixtures made with 0.5% and 1.0% PVA fibers, respectively. Such flowability reduction was due to the presence of fibers that can restrict the movement of sand and increase viscosity. However, compared to the additional fibers, the use of WCR led to a larger reduction in mini-slump flow. With the use of 30% and even 60% waste rubber, the mini-slump flow was reduced by 10% and 23%, respectively, regardless of the fiber content in the PVA-FRRM. It is worth noting that the dropping was much lower compared to the approximately 50%–60% reported in the literature [42,43]. This was since the hydrophobic nature of WCR, which adversely affects flowability, can be effectively improved by the LTP treatment.

The density of PVA-FRRM mortars was not affected significantly by the incorporation of PVA fibers, while the addition of WCR significantly reduced density. When the substitution rate of WCR reached 60%, the density of the R60P1.0 mortar was 1.947 g/cm^3.

3.2. Static mechanical properties

It is widely accepted that the incorporation of waste rubber can considerably reduce mechanical properties [19]. In this study, the presence of PVA fiber and the LTP pre-treatment method of the WCR particles were shown to compensate for some of these disadvantages. Fig. 10(a) shows the flexural strength of seven mortars which indicates that the fiber addition can effectively increase the flexural strength, while the WCR substitution of sand had a negative effect on flexural strength. A maximum increase of 42% in flexural strength was observed by the use of 1.0% PVA fiber compared to the reference mortar. Such an increase was 29% for the mortar with 0.5% fiber. This enhancement can be attributed to the bridging effect caused by the PVA fiber in the FRM. In addition, even though the WCR particles were pre-treated by the LTP method, a 30% WCR replacement caused an 18% reduction in flexural strength. With increasing the WCR replacement to 60% in the PVA-FRRM, the flexural strength showed a drop of 36%. However, due to the strength increase provided by the combination of PVA fibers and pre-treatment of the WCR, the R60P1.0 mortar exhibited a higher flexural strength of 6.3 MPa than the reference mortar.

It can be also seen in Fig. 10(b) that the fiber addition also contributed to the improvement of compressive strength, while the WCR replacement of sand yielded the opposite effect. The slight contribution of fiber content for enhanced compressive strength is due to the restriction of crack development and providing lateral restraint, even at the low fiber volume. Increases in compressive strength of 4% and 11% were observed with the addition of 0.5% and 1.0% of fibers, respectively. However, the compressive strength still decreased when the WCR substitution increased, regardless of the fiber content in the PVA-FRRM. Compared to the RP1.0 mortar, the addition of 30% WCR led to a 14% reduction in compressive strength, and a greater drop of 27% was observed at a 60% replacement rate. Qaidi [44] reported a reduction in compressive strength of 20%–70% was obtained in rubber-containing mortars prepared with 15%–60% replacement of WCR particles, by volume, respectively. The major reasons for this drop were attributed to the poor adhesion between the recycled rubber and cement-FA matrix caused by the hydrophobic nature and smooth surface of the rubber. The LTP treatment of the WCR particles alleviated these two deficiencies. Such treatment coupled with the use of PVA fibers reduced even further any drop in compressive strength of the PVA-FRRMs.

3.3. Material damping characteristics

3.3.1. Dynamic stiffness

The distinct difference between static and dynamic stiffness is the applied force. The ability to resist deformation under dynamic loads is called dynamic stiffness, which is the dynamic force required to induce a unit amplitude. If the disturbance force changes very slowly, the dynamic stiffness is basically the same as the static stiffness. When the frequency of this disturbance force is much greater than the natural frequency of the concrete structure, the structural deformation is relatively small, that is, the dynamic stiffness is relatively large. In this study, the dynamic stiffness of seven mortars was measured by the DTMA test under given experimental conditions, and the corresponding theoretical consideration is illustrated in Table 4. Considering the tight attachment between the test sample and the compression plate provided by the glue and confining pressure, the hypothesis diagram on deformation under dynamic load can lead to some distortion of the test

Table 4
Theoretical consideration for Young's modulus and dynamic stiffness under the compression mode of DTMA test.

Theoretical formula	Hypothesis on deformation
$E' = \frac{Kh}{S_e} \times F_c \times \cos\delta, F_c = \frac{1}{1+2\left(\frac{S_e}{S_l}\right)^2}$ where: E' = real part of Young's modulus K = sample stiffness h = sample height S_e = excitation area F_c = shape correction factor S_l = side area δ = phase angle	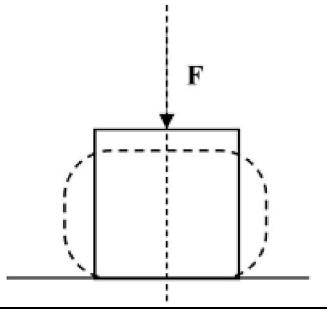

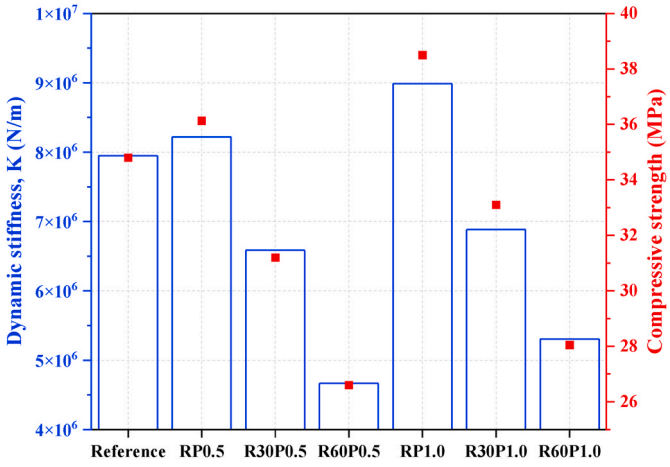

Fig. 11. The relationship between dynamic stiffness and compressive strength of sustainable FRMs and PVA-FRRMs.

sample. Such distortion on the sample can result in a complex stress field within the material. A correction factor related to the sample shape is then considered in the theoretical analysis to reflect the real part of Young's modulus and stiffness.

Based on the measurement protocol of the DTMA test of a vibration frequency of 0.5 Hz and room temperature, the relationship between the dynamic stiffness and compressive strength of the seven test mortars is summarized in Fig. 11. Overall, the effects of fiber volume and WCR replacement on dynamic stiffness were consistent with the results of compressive strength. With increasing fiber volume, the dynamic stiffness increased by 13% compared to the reference mortar, from 8×10^6 to 9×10^6 N/m. However, a considerable reduction was observed with the WCR substitution. This can be due to the great disparity in Young's modulus of viscoelastic rubber compared to the cement-FA matrix, which can be considered a major reason for strength reduction. With the use of 1% fiber in the PVA-FRRM, the dynamic stiffness decreased by 42% when the WCR substitution rate increased to 60%.

To clarify the effect of fiber incorporation along with WCR on the dynamic stiffness under different frequencies (0.5, 1.0, 1.5, and 2.0 Hz), the variations of dynamic stiffness of the seven mortars with excitation time are shown in Fig. 12. In general, the upward and downward trends with time for the seven mortars at four distinct frequencies were similar; however, most notably the value of dynamic stiffness at 0.5 Hz was the highest, and the remaining three frequency points had basically unchanged dynamic stiffnesses. Thus, it can be concluded that the test mortars can obtain the best resistance to deformation under 0.5 Hz vibration frequency (i.e., vehicle loads on roads and track loads on sleepers). Moreover, the fiber incorporation contributed to the increase of dynamic stiffness, while the WCP replacement led to an adverse effect, regardless of fiber content in the PVA-FRRMs.

The variation of dynamic stiffness of the mortars remained stable in the initial 30 min. However, with excitation time elapsing (exact phase in temperature history of −30 °C–50 °C), significant amplitude change shown in the gray background indicates temperature sensitivity towards dynamic stiffness, which is further described in Section 3.3.4.

3.3.2. *Dynamic modulus and energy transfer*

The dynamic modulus refers to the ratio of the dynamic stress to the dynamic strain under a given load cycle with the time lag of a test material subjected to sinusoidal vibration. The dynamic modulus includes the storage modulus and loss modulus in the DTMA test. The former is the real part and represents the rigidity of an elastic component, while the latter is the imaginary part and represents the viscous component of the material. The storage modulus is generally related to Young's modulus. It is usually associated with a material's stiffness and is considered the tendency of a material to store energy. In contrast, the loss modulus is a viscous response of the material and is viewed as the ability of a material to dissipate energy applied on it [29]. In this study, the dynamic modulus and energy transfer of the seven test mortars under four specific frequencies of 0.5, 1.0, 1.5, and 2.0 Hz were evaluated.

Fig. 13(a) and (b) illustrate the detailed results of the storage modulus and loss modulus, respectively. Overall, when subjected to a vibration frequency of 0.5 Hz, the dynamic modulus of mortars presented the highest value, regardless of the fiber volume and WCR replacement, most notably in the loss modulus. There was a downward creep at a vibration frequency of 1.0 Hz, followed by a stable trend as the frequency increased. The 0.5 Hz frequency was the most optimum vibration frequency in the low-frequency range. In addition, it can be observed that the FRMs had a higher dynamic modulus. This is consistent with the results of the improved compressive strength brought by the incorporation of fibers. The presence of bridging effects under load cycles contributed to the dynamic stiffness of the mortar, while the PVA fibers provided the viscous components. With the use of 0.5% PVA fiber at 0.5 Hz, the storage and loss modulus of the FRM increased by 2.5% and 30%, respectively. When the fiber volume increased to 1.0%, the dynamic modulus had the highest values among all seven mortars. However, the use of WCR reduced the dynamic modulus. With the increase in the substitution rate of WCR, there was a considerable drop in the dynamic modulus. The lowest storage and loss modulus of 2.07×10^8 and 1.28×10^7 MPa were obtained in the PVA-FRRM with 60% WCR and reduced by 43% and 34%, respectively, compared to the FRM made without any waste rubber. This can be attributed to the weak interface transition zone (ITZ) between the rubber and cement-FA matrix. The presence of PVA fiber provided the increased dynamic modulus of the PVA-FRRM, especially in the case of the loss modulus. The addition of 0.5% fiber compensated for 28% of the loss modulus in the PVA-FRRM made with 60% treated WCR and even surpassed the reference mortar.

During a load cycle, the storage modulus is proportional to the maximum energy stored, while the loss modulus is proportional to the energy dissipated. Fig. 13(c) and (d) show the energy transfer including energy absorption and dissipation of seven mortars under the same frequency conditions (0.5, 1.0, 1.5, and 2.0 Hz). The increase of the fiber volume did not ameliorate the energy absorbed ability of the FRM, when incorporating 1% fiber, there was a 9% reduction in energy absorption at 0.5 Hz. Instead, fiber addition contributed to dissipating 35% of energy during a load cycle. This was due to the energy conversion transferred from the vibrational potential energy into mechanical energy in the form of fiber deformation; however, incorporating fibers reduced the matrix's ability to store energy by creating multiple micro-interfaces that affected the rigidity of the matrix, which lead to lower energy absorption [29]. In addition, due to the favorable viscoelasticity of the WCR particles, the substitution of WCR is beneficial in absorbing and dissipating energy. A considerable increase of 69% and 148% in energy

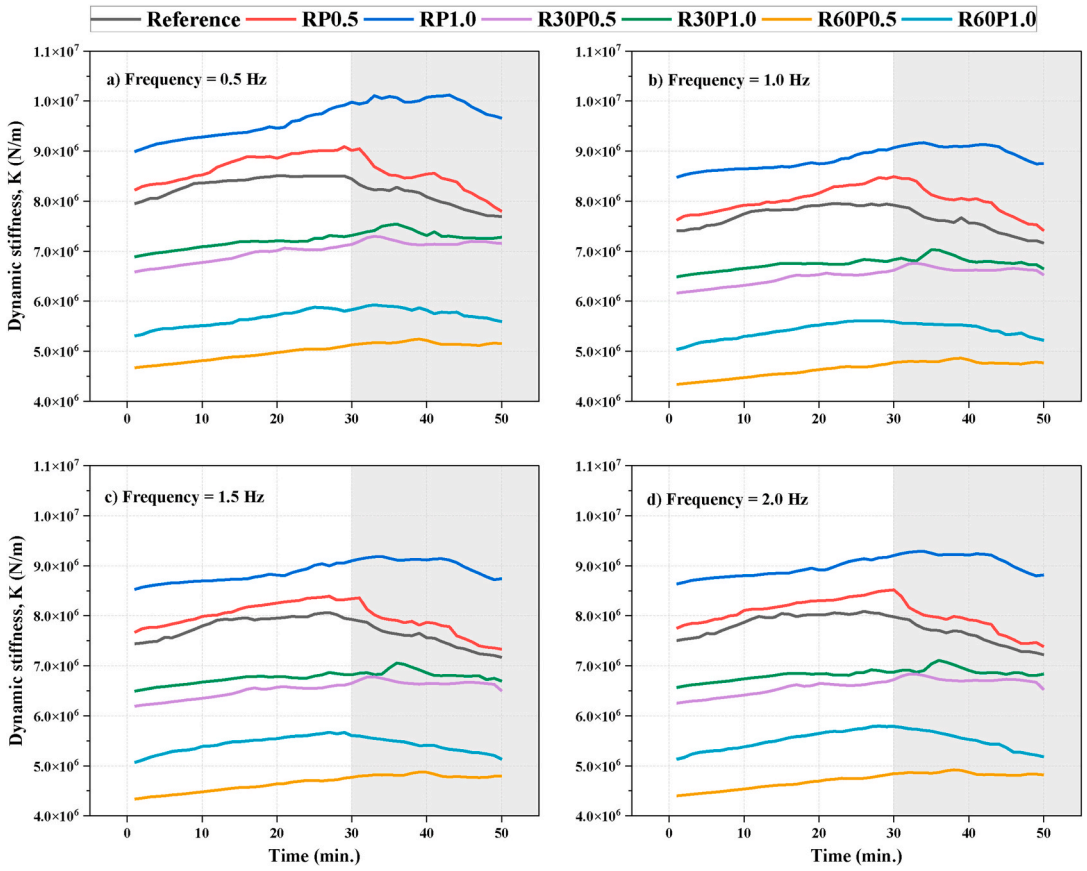

Fig. 12. Dynamic stiffness of sustainable FRMs and PVA-FRRMs with testing time collapse at four different vibration frequencies. a) 0.5 Hz; b) 1.0 Hz; c) 1.5 Hz; and d) 2.0 Hz.

absorption and dissipation at 0.5 Hz was obtained with the combination of 60% WCR and 0.5% fiber, respectively, compared to the reference mortar. However, in the PVA-FRRMs, the increase in fiber volume had an insignificant influence on energy absorption when incorporated with 30% WCR substitution. Moreover, it did not improve energy dissipated ability while there was 60% of WCR. This can be hypothesized that the energy transfer of the PVA-FRRMs depended on the combination of fiber and WCR. When the WCR content was only 30%, the fiber led to dissipation in energy, but once the content increased to 60%, the presence of waste rubber dominated the energy dissipation process in the PVA-FRRM under vibration.

3.3.3. *Material damping characteristics*

The loss factor (tanδ) can be used as a measure of the damping of a viscoelastic system and reflects its capacity to dissipate mechanical energy into heat. The tanδ is the ratio of the loss modulus over the storage modulus, as follows:

$$\tan \delta = E''/E'$$

where δ is the phase angle, E″ is the loss modulus, and E′ is the storage modulus. A value of 0.025–0.051 is a common loss factor range of cracked concrete [45]. Cement-based materials are traditional composite materials with relatively high stiffness and moderately low material damping. Such key factors including the composite components, moisture content, curing age, temperature, and relative humidity can affect the material damping [46]. In this study, the damping characteristics of the seven investigated mortars under different vibration frequency conditions were evaluated by determining the loss factor and energy dissipating ratio, as shown in Fig. 14.

Material damping of the FRMs and PVA-FRRMs improved with the addition of PVA fibers and combined with viscoelastic WCR particles. With increasing fiber volume to 0.5% and 1.0%, the energy dissipating ratio of the FRM improved by 27% and 40% with a higher loss factor at 0.5 Hz. This suggests that the use of synthetic fiber with low modulus helps dissipate energy under load cycles. Moreover, the combination of WCR and PVA fibers dramatically improved the material damping characteristics. The loss factor and energy dissipating ratio of the PVA-FRRMs increased sharply when incorporating WCR and PVA fiber. As one of the main viscous components, WCR undertook the foremost energy-consuming role, most notably in the high substitution rate. The R60P1.0 mortar made with 60% WCR and 1.0% fiber had the highest loss factor and energy dissipating ratio of 0.07 and 0.44, and it increased by 65% and 63%, respectively, compared to the reference mortar.

Fig. 14(c) clearly illustrates the combined effect of fiber content and WCR replacement on the reinforcement ratio of the loss factor under four frequencies (0.5, 1.0, 1.5, and 2.0 Hz). The reinforcement ratio refers to the damping efficiency and can be expressed as a ratio to the loss factor of the reference mortar. It can be observed that the reinforcement ratio was the highest at 0.5 Hz in the low-temperature range, regardless of the fiber content and WCR replacement. Combined with the results of dynamic stiffness and dynamic modulus under the same frequency conditions, it can be also concluded that 0.5 Hz was the most optimized frequency in which the highest damping properties can be obtained under the load cycle. Pure fiber reinforcement at only 0.5% and 1.0% volume contributed to a 20%–35% increase in the loss factor. The combination of the fiber content and WCR replacement favored increases of 28.7%–64.8%, while the R60P1.0 mortar with 60% WCR and 1.0% fiber exhibited the highest reinforcement ratio of 65% at 0.5 Hz.

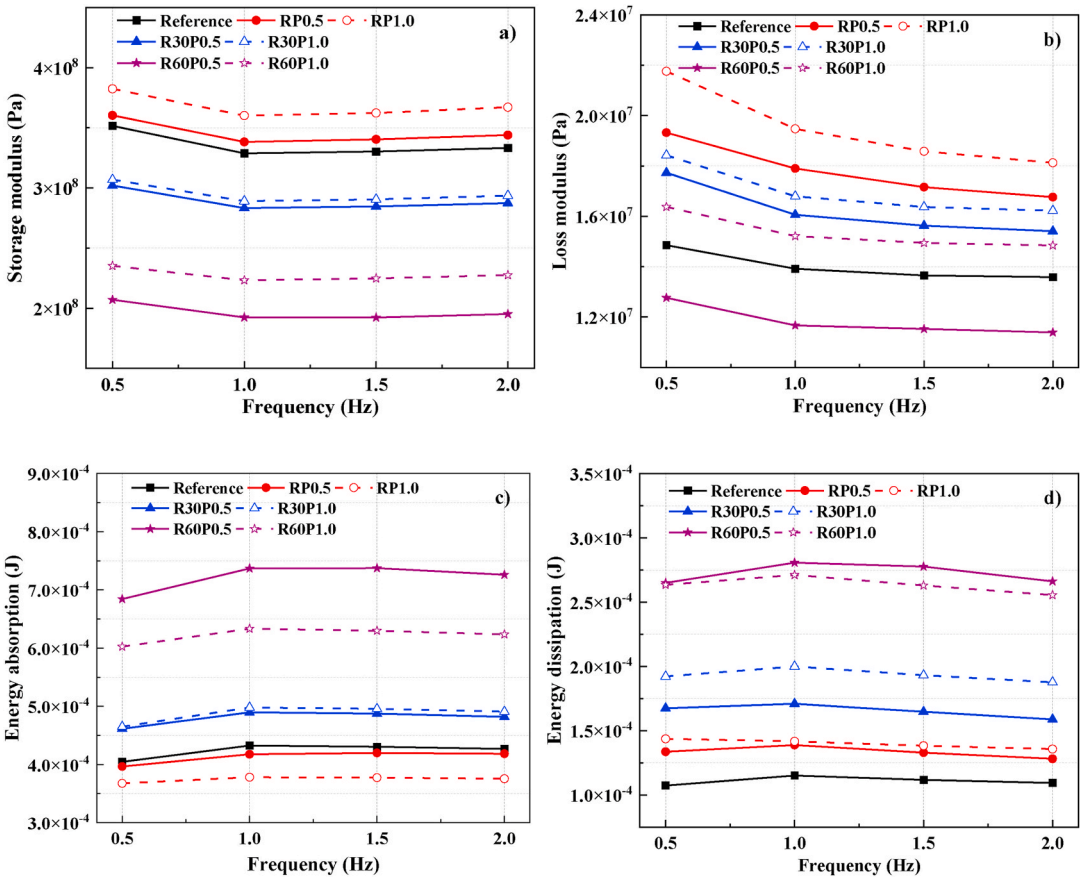

Fig. 13. Dynamic modulus and energy transfer of sustainable FRMs and PVA-FRRMs under multiple vibration frequency conditions (0.5–2 Hz). a) Storage modulus; b) Loss modulus; c) Energy absorption; and d) Energy dissipation.

3.3.4. Effect of excitation temperature on dynamic modulus and loss factor

The conditioning temperature is one of the key factors affecting the material damping of cement-based composites. Based on the given frequency/temperature superposition and established temperature profile (−30 to 50 °C), the effect of the excitation temperature ramp on the loss modulus, storage modulus, and loss factor of the seven test mortars was investigated.

Fig. 15 illustrates the results of the dynamic modulus under multiple temperature stages (room temperature, cold temperature, zero temperature, and hot temperature) at 0.5 Hz. The temperature protocol was divided into two processes, cooling and heating processes from room temperature to −30 °C and −30 °C–50 °C, respectively. During the cooling process in the initial temperature setpoints (shown in Fig. 15(a) and (c)), the loss modulus of all FRMs and PVA-FRRMs showed a slight downward trend, while the storage modulus showed an opposite uptrend. This status involves the phase change of free water around the pores in the cement-FA matrix, which goes through the freezing of the capillary water. The improved stiffness of solid ice contributes to the increase in the storage modulus; however, the viscous degree was weakened. In addition, the variations of the dynamic modulus of the test mortars with the temperature profile were similar to the effects of changing the vibration frequency. Thus, the combined effect of fiber content and WCR replacement on the dynamic modulus was not affected regardless of the multi-vibration frequency or multi-excitation temperature. Switching to the heating process when subjected to measured temperature ranges of −30 °C–50 °C, as shown in Fig. 15(b) and (d). Such an increase in temperature at a fixed frequency can result in an increase in free volume and movement of channels of thermal origin; this is conveyed by a slight decrease in the dynamic modulus. There was a significant difference that can be observed in the dynamic modulus, especially at temperature setpoints of 0 and 50 °C, which indicated the regulated fluctuations. When subjected to the iso-temperature of 0 °C, the storage and loss modulus of all test mortars presented a sharp drop. This can be explained that parts of frozen water are thawed and back to the liquid state; as a result, the expansive stress generated by ice will be mitigated. While the temperature behavior at the higher level had little difference, except for the loss modulus at a single temperature setpoint of 50 °C. This leap at 50 °C can be defined as the transition temperature, which can reveal a sharp increase in dynamic modulus.

The loss factor of the seven investigated mortars on the same freeze-high temperature span is shown in Fig. 16. Basically, the varied trends related to the effects of fiber content and WCR replacement on both cooling and heating temperature ranges were similar, which were also consistent with the previous results of loss factor towards the vibration frequency. Such a considerable increase in loss factor was provided by the combination of PVA fibers and treated WCR, which improved the material damping regardless of the excitation temperature or vibration frequency. However, in the cooling process, the loss factor showed a decrease when the temperature decreased. This can be attributed to the varied moisture contents in the mortars, which is the key factor determining the viscous components. The lower moisture content in the mortar due to some transformation into ice at low temperatures resulted in poor damping ability at cold temperatures. While in the heating process, there was a stable increase when the temperature increased, except for at the two iso-temperatures of 0 °C and 50 °C. There are also two vertical fluctuations, one was a drop at 0 °C while the other was a surge at 50 °C.

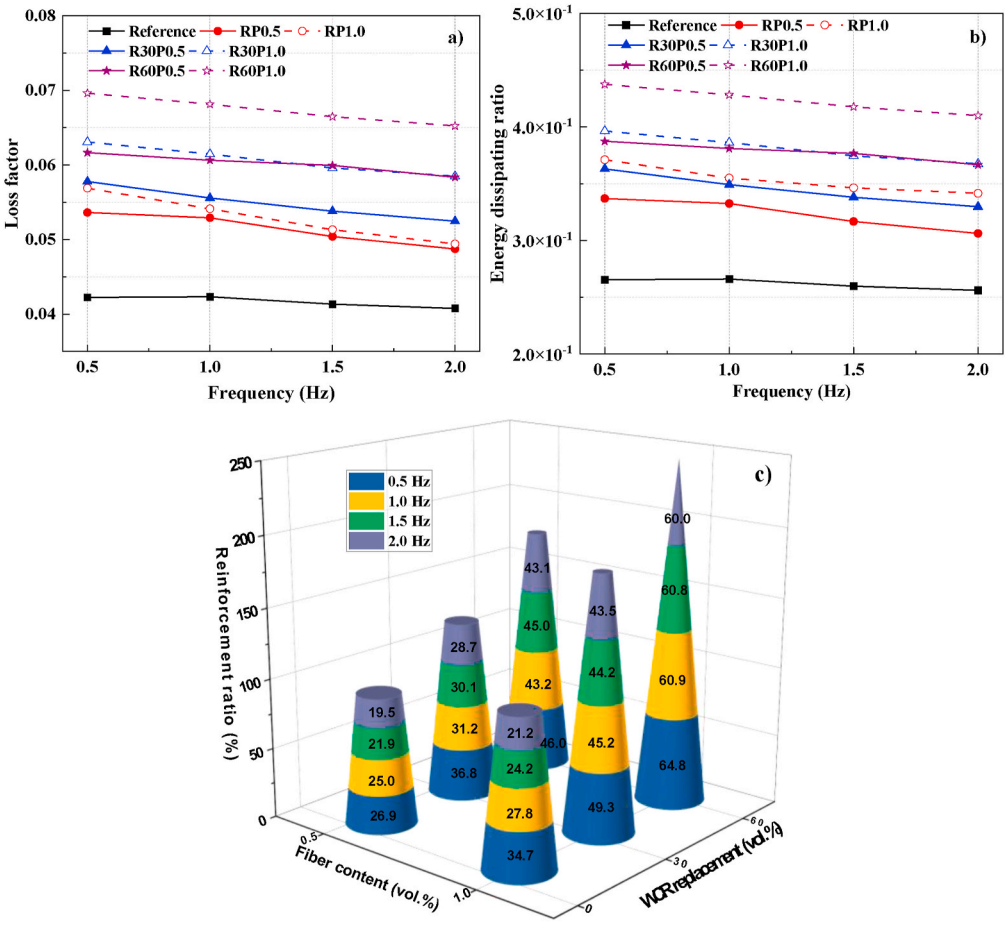

Fig. 14. Damping and energy dissipating ratio of sustainable FRMs and PVA-FRRMs under multiple frequencies conditions (0.5–2 Hz). a) Loss factor; b) Energy dissipating ratio; and c) Reinforcement ratio concerning fiber contents and WCR replacements.

3.4. Microscopic characterization

The micro-level structures of the cement-FA matrix have a large impact on the material damping, most notably for the pore structure and micro-ITZ. The increase of pores is mainly beneficial to the energy dissipation of internal friction during vibration [47]. And improving the ITZs in the cement-FA matrix, such as replacing low-stiffness aggregates to weaken the interface or introducing micro-nano particles to form a large number of micro-interfaces, can significantly enhance the material damping [48,49].

The effect of fiber content and treated WCR on the porosity and pore volume fraction of FRMs and PVA-FRRMs at 28 days is demonstrated in Fig. 17. The pores in the cement-FA matrix can be divided into four categories according to the apparent pore diameters: i) gel micropores (<0.01 μm), ii) mesopores (0.01–0.1 μm), iii) capillary pores (1–10 μm), and iv) large pores (>10 μm) [50]. Fig. 17(a) illustrates the cumulative porosity volume increase with the fiber volume. Moreover, increasing the WCR addition in the PVA-FFRMs further increased the cumulative porosity. The combination of 1.0% PVA fibers and 60% WCR presented nearly the highest cumulative porosity volume. This can be attributed to the relatively weak interface introduced by fiber and WCR additions. The increased porosity can in turn adversely affect mechanical properties while increasing the material damping characteristics of mortar. Furthermore, the pore volume fraction of the FRM and PVA-FRRM under the four classified pores is shown in Fig. 17(b). On the left side, increasing the PVA fiber volume at low levels is shown to improve mesopores but increase the volume of the large pores. Moreover, the volume fraction of the gel and capillary pores was unchangeable. Incorporating fibers would introduce entrained air and fiber-matrix interfaces, which leads to a higher volume of large pores in the mortar. This can be also attributed to the increased material damping made with the relatively low fiber volume. While the WCR addition significantly affected the pore size distribution of the PVA-FRRMs. No matter the gel pores or mesopores, their volume fractions were both reduced due to the incorporation of treated WCR. However, the presence of WCR further increased the large pore volume and there was a 53% increase when incorporating 60% WCR, compared to that of the RP1.0 mortar made without any WCR. This proves again the negative effect of WCR on the pore structure of the mortars, which reversely improves the material damping characteristics due to the greater energy dissipation provided by the increased pores in the cement-FA matrix.

The micro-morphologies of the PVA-FRRM incorporated with the 60% treated WCR at 28 days after conducting the DTMA test are shown in Fig. 18. Unreacted FA and hydration products including flocculated *C*–S–H gels, hexagonal $Ca(OH)_2$ flakes, and rod-like AFt can be found in Fig. 18(a) and (b). These reactants provided "filling-effect" and nucleation sites for the mesocracks where energy can be dissipated by Coulomb friction, which contributed further to dissipating energy during vibration [51]. This assures that the increased damping capacity can be produced without significant strength or stiffness loss. As shown in Fig. 18(c), there shows a full view of the cement-FA matrix including dispersed PVA fibers, waste rubber, and a small number of pores. After magnification in Fig. 18(d), a tight rubber-matrix interface and a relatively loose fiber-matrix interface with a ruptured end and fibrillations can be clearly presented. These features can contribute to energy dissipation when subjected to dynamic loading through the conversion of mechanical energy. In addition, the microstructural morphology of plasma-treated waste rubber and its interface in the cement-FA matrix

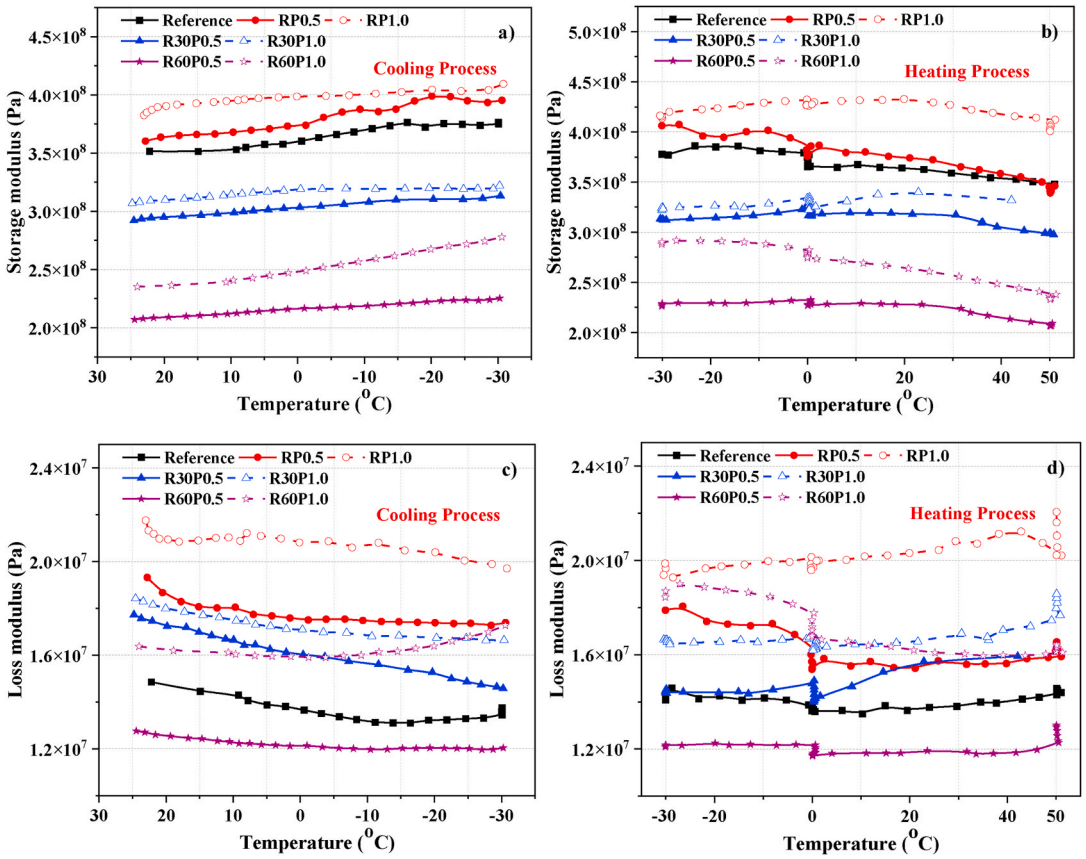

Fig. 15. Dynamic modulus of sustainable FRMs and PVA-FRRMs under multiple temperature conditions (-30–50 °C). a) and b) Storage modulus on cooling and heating process; c) and d) Loss modulus on cooling and heating process.

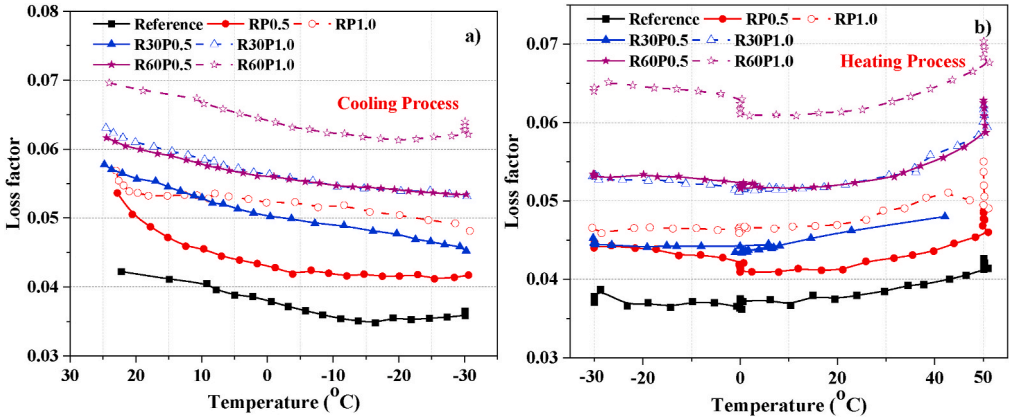

Fig. 16. Damping of sustainable FRMs and PVA-FRRMs under multiple temperature conditions (-30–50 °C). a) Loss factor on cooling process; b) Loss factor on the heating process.

can be seen in Fig. 18(e) and (f). The treated WCR showed a slightly rough surface and there was a relatively tight mesocrack in the rubber-matrix interface, which indicates the effectiveness of the LTP treatment. This is also consistent with the results of improved material damping without a considerable strength loss.

3.5. Mechanism hypothesis

3.5.1. Effect of viscous damping hysteresis on material damping

Normally, incorporating WCR particles inherent with organic components into inorganic cement-based materials is hard to balance the improved ductility and reduced strength. Although the toughness of cement composites incorporated with WCR can be effectively ameliorated, the introduced weak bond between the low-modulus rubber and cement matrix is the major cause undermining their compressive and flexural strength proportion.

In this study, given the beneficial modification of LTP pre-treatment, the alleged weak bonding can be modified as shown by SEM results, and therefore the considerable loss of strength can be compensated. Most importantly, the dynamic mechanical properties including damping and energy dissipation were effectively improved while dynamic modulus was diminished with the use of WCR regardless of the test frequency and

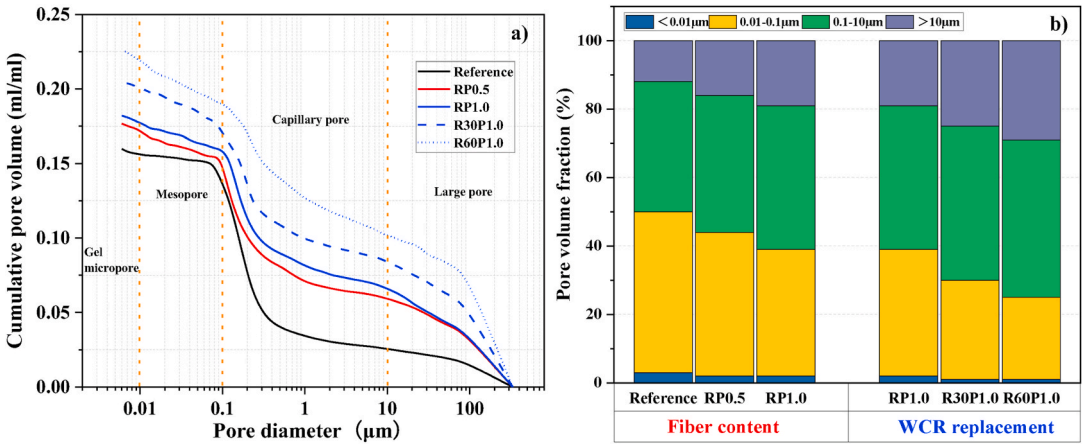

Fig. 17. MIP analysis results of parts of sustainable FRMs and PVA-FRRMs concerning fiber contents and WCR replacements.

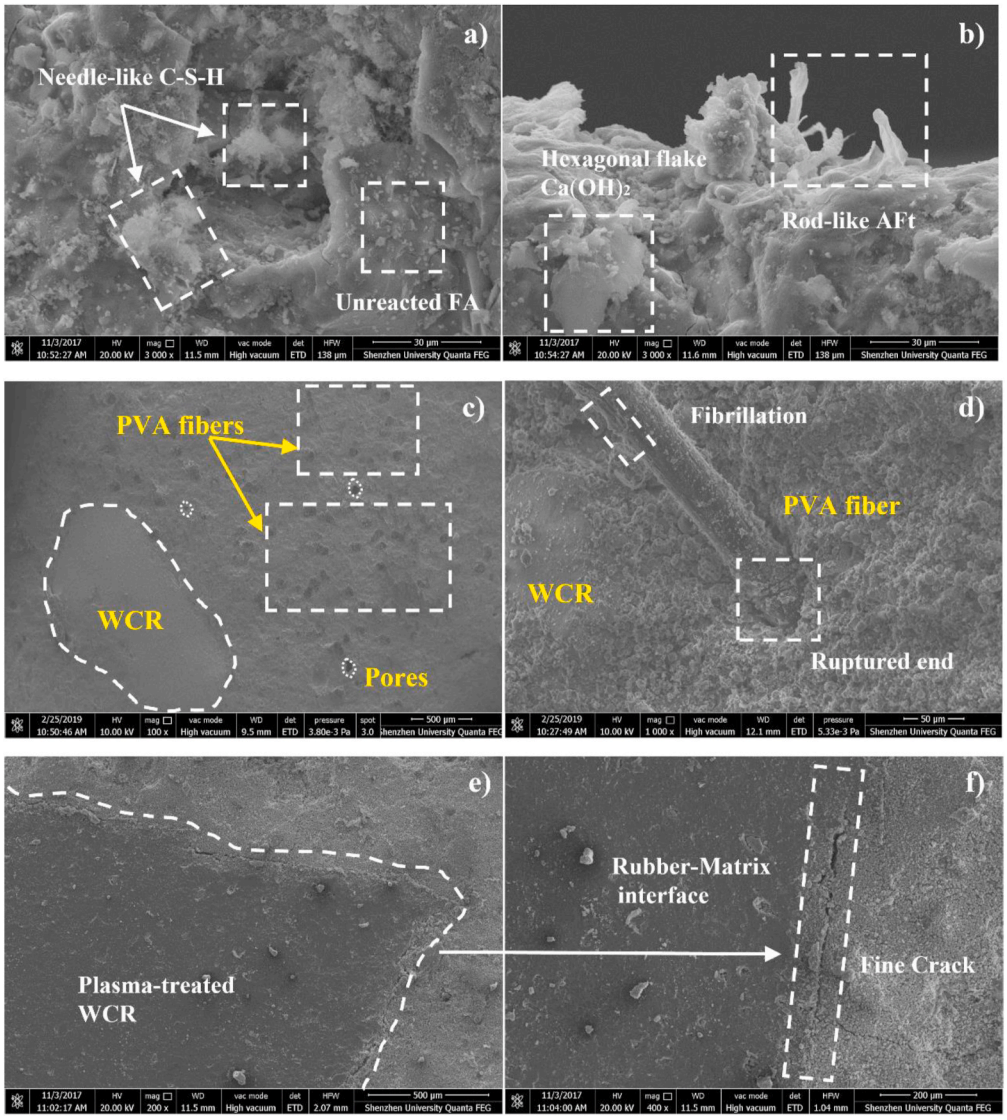

Fig. 18. SEM micromorphology of the PVA-FRRM incorporated with 60% WCR particles at 28 days.

temperature. This can be explained by the viscous damping hysteresis brought by the rubber material. Some delay occurs due to viscous components of the WCR with regard to strain inconsistency under the applied sinusoidal vibration force. The relative movement between the softer WCR and harden cement-FA matrix is beneficial to dissipating energy. In addition, vibrational energy may be transferred through the opening and closing of fine cracks in these introduced ITZs [52].

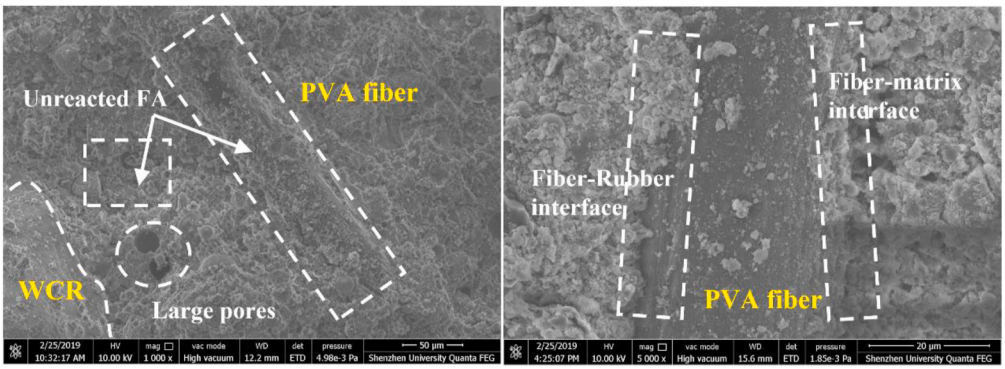

Fig. 19. Cross section of PVA fiber-matrix and fiber-rubber interfaces.

3.5.2. Effect of interfacial coulomb friction on material damping

The fiber reinforcement at low PVA fiber volume can induce a profound influence on dynamic properties. Such fiber alignment substantially improved the material damping characteristics and the dynamic modulus for the FRMs and PVA-FRRMs. Interfacial Coulomb friction can be regarded as the main explanation due to the viscoelastic nature of the PVA fibers, which essentially have greater damping capacity compared to the cement-FA matrix. When the PVA fibers yielded under the loading cycles, fibrillations on the surface and their ruptured ends (shown in Fig. 18(d)) were able to partially dissipate energy through inconsistent strain effects. This can effectively alleviate stress concentration in the cement-FA matrix, thus improving material damping characteristics. In addition, the relatively loose adhesion (also shown in Fig. 19) without detectably attached hydration products between the fiber and cement-FA matrix may give rise to the relative interface slip, which contributes to energy dissipation and damping capacity under the dynamic loading. This results from the contingent fiber debonding when the vibrational stress amplitude is greater than the interfacial bond strength. It was reported that a lower aspect ratio of the synthetic fiber can be advantageous for such sort of fiber debonding during the vibration leading to a higher damping capacity [53].

3.5.3. Effect of porosity and interface transition zone on material damping

The improved damping mechanisms induced by the corresponding porous changes and interface function are explained in detail. Due to the addition of PVA fibers and WCR, the total cumulative pore volume of PVA-FRRM increased, especially for the proportions of large pores and connective capillary pores. This can result in large amounts of microflaws in the cement-FA matrix, which is attributed to the transfer of the vibrational energy by mechanical works in the form of opening and closing when subjected to the load cycles. Moreover, redundant connective pores helped form desirable energy dissipation channels and further facilitated dissipating vibrational energy and thus improved damping capacity [29].

Idealized dampening interfaces are prone to generate while introducing low stiffness aggregate, micro-particles like silica fume [54], or nanomaterials like graphite with the network structure [55]. In this study, the addition of softer WCR and viscous PVA fibers results in organic-inorganic and organic-organic interfaces at the same time. Fig. 18 illustrates the microstructural morphology of the ITZ of the PVA-FRRM cross-section. There coexisted unreacted FA due to the poor pozzolanic activity of FA, large pores, microcracks, WCR-matrix interface, and PVA fiber attached large amounts of unreacted FA in cement-FA matrix. It is approved that the stiff matrix combined with viscoelastic aggregates can promote the damping capacity due to their internal defects and dislocations, which are related to the energy dissipation of vibrational friction [56]. The ITZ of the rubber matrix can be considered an interlocking interface that resembled the sandwich structure. This is an energy-dissipating pattern in which the viscoelastic layer was surrounded by two identical elastic layers. Moreover, unreacted FA micro-particles attached to the PVA fiber further enhanced the frictional sliding between fiber-matrix interfaces and thus upgraded the material damping. In addition, the presence of fiber-matrix and fiber-rubber interfaces can be hypothesized as energy-dissipating channels [29]. The relative friction and crack propagation in these channels can consume part of the vibrational energy under cyclic loading.

4. Conclusion

Given the increasing demand for eco-efficiency and structural-functional integration, a sustainable fiber-reinforced rubber mortar using WCR, PVA fibers, and HVFA was successfully developed with superior damping characteristics. Static and dynamic mechanical tests, coupled with the micro characterization of pore structures and micromorphology of PVA-FRRM led to the following conclusions.

- LTP pre-treatment was shown to be effective to alter the inherently hydrophobic nature of the WCR. The contact angle test showed both left and right contact angles increased to 119.4° and 118.5° from 74.4° and 75.2°, respectively.
- HVFA system offered favorable workability in FRMs and PVA-FRRMs; however, the addition of PVA fiber and WCR induced an unreversible workability loss, most notably when combining 60% WCR and 1% PVA fiber. Although the use of 60% WCR resulted in a 36% and 27% reduction in flexural and compressive strengths, respectively, these deficiencies can be desirably mitigated by using PVA fibers and LTP pre-treatment.
- The combination of PVA fibers and viscoelastic WCR showed excellent damping capacity and energy dissipating ratio during cyclic loading. The R60P1.0 mortar with 60% WCR and 1.0% PVA fiber exhibited the highest reinforcement ratio of 65% in loss factor at 0.5 Hz. In addition, no matter when subjected to multi-frequencies or multi-temperatures, the improved trend for dynamic mechanical properties of the sustainable PVA-FRRMs with the optimized combination was quite similar.
- MIP and SEM tests indicated that the addition of WCR and PVA fiber affected the pore size distribution and resulted in a greater volume of large pores and interfaces in the cement-FA matrix, which can be considered effective ways of dissipating energy during vibration.

Declaration of competing interest

The authors declare that they have no known competing financial interests or personal relationships that could have appeared to influence the work reported in this paper.

Data availability

Data will be made available on request.

Acknowledgments

The authors gratefully acknowledge the financial support provided by the Guangdong Provincial Key Laboratory of Durability for Marine Civil Engineering at Shenzhen University (No. 2020B1212060074), as well as the Clayco Advanced Construction and Material Laboratory (ACML) and Center for Infrastructure Engineering Studies (CIES) at Missouri University of Science and Technology.

References

[1] National Annual Report on the Prevention and Control of Solid Waste Pollution in Large and Medium Cities, 2020.
[2] S.C. Guo, Q.L. Dai, R.Z. Si, X. Sun, C. Lu, Evaluation of properties and performance of rubber-modified concrete for recycling of waste scrap tire, J. Clean. Prod. 148 (2017) 681–689.
[3] A. Siddika, M.A.A. Mamun, R. Alyousef, Y.H.M. Amran, F. Aslani, H. Alabduljabbar, Properties and utilizations of waste tire rubber in concrete: a review, Construct. Build. Mater. 224 (2019) 711–731.
[4] R. Roychand, R.J. Gravina, Y. Zhuge, X. Ma, O. Youssf, J.E. Mills, A comprehensive review on the mechanical properties of waste tire rubber concrete, Construct. Build. Mater. 237 (2020), 117651.
[5] M.M. Islam, J. Li, R. Roychand, M. Saberian, F.J. Chen, A comprehensive review on the application of renewable waste tire rubbers and fibers in sustainable concrete, J. Clean. Prod. 374 (2022), 133998.
[6] W.J. Long, H.D. Li, J.J. Wei, F. Xing, N.X. Han, Sustainable use of recycled crumb rubbers in eco-friendly alkali activated slag mortar: dynamic mechanical properties, J. Clean. Prod. 204 (2018) 1004–1015.
[7] A. Bala, S. Gupta, Thermal resistivity, sound absorption and vibration damping of concrete composite doped with waste tire Rubber: a review, Construct. Build. Mater. 299 (2021), 123939.
[8] N.N. Gerges, C.A. Lssa, S.A. Fawaz, Rubber concrete: mechanical and dynamical properties, Case Stud. Constr. Mater. 9 (2018), 100184.
[9] B.D. Liu, S.Z. Yang, W.L. Li, M.Q. Zheng, Damping dissipation properties of rubberized concrete and its application in anti-collision of bridge piers, Construct. Build. Mater. 236 (2020), 117286.
[10] X.C. Mei, Q. Sheng, Z. Cui, M.C. Zhang, D. Dias, Experimental investigation on the mechanical and damping properties of rubber-sand-concrete prepared with recycled waste tires for aseismic isolation layer, Soil Dynam. Earthq. Eng. 165 (2023), 107718.
[11] A.A. Aliabdo, A.E.M.A. Elmoaty, M.M. AbdElbaset, Utilization of waste rubber in non-structural applications, Construct. Build. Mater. 91 (2015) 195–207.
[12] C.Y. Lin, G.C. Yao, C.H. Lin, A study on the damping ratio of rubber concrete, J. Asian Architect. Build Eng. 9 (2010) 423–429.
[13] F. Aslani, Mechanical properties of waste tire rubber concrete, J. Mater. Civ. Eng. 28 (2016) 1–14.
[14] N.P. Pham, A. Toumi, A. Turatsinze, Rubber aggregate-cement matrix bond enhancement: microstructural analysis, effect on transfer properties and on mechanical behaviours of the composite, Cem. Concr. Compos. 94 (2018) 1–12.
[15] I. Marie, Zones of weakness of rubberized concrete behavior using the UPV, J. Clean. Prod. 116 (2016) 217–222.
[16] D. Li, Y. Zhuge, R. Gravina, J.E. Mills, Compressive stress strain behavior of crumb rubber concrete (CRC) and application in reinforced CRC slab, Construct. Build. Mater. 166 (2018) 745–759.
[17] K. Rashid, A. Yazdanbakhsh, M.U. Rehman, Sustainable selection of the concrete incorporating recycled tire aggregate to be used as medium to low strength material, J. Clean. Prod. 224 (2019) 396–410.
[18] F.M. Ren, J.X. Mo, Q. Wang, J.C.M. Ho, Crumb rubber as partial replacement for fine aggregate in concrete: an overview, Construct. Build. Mater. 343 (2022), 128049.
[19] R.A. Assaggaf, M.R. Ali, S.U. Al-Dulaijan, M. Maslehuddin, Properties of concrete with untreated and treated crumb rubber - a review, J. Mater. Res. Technol. 11 (2021) 1753–1798.
[20] R.Z. Si, S.C. Guo, Q.L. Dai, Durability performance of rubberized mortar and concrete with NaOH-Solution treated rubber particles, Construct. Build. Mater. 153 (2017) 496–505.
[21] M. Ateeq, A. Ai-Shamma'a, Experimental study on the microwave processing of waste tyre rubber aggregates to enhance their surface properties for their use in rubberized bituminous mixtures, Microw. Opt. Technol. Lett. 59 (2017) 2951–2960.
[22] O. Onuaguluchi, Effects of surface pre-coating and silica fume on crumb rubber-cement matrix interface and cement mortar properties, J. Clean. Prod. 104 (2015) 339–345.
[23] X.W. Cheng, D. Long, S. Huang, Z.Y. Li, X.Y. Guo, Time effectiveness of the low-temperature plasma surface modification of ground tire rubber powder, J. Adhes. Sci. Technol. 29 (2015) 1330–1340.
[24] X.W. Cheng, S. Huang, X.Y. Guo, W.H. Duan, Crumb waste tire rubber surface modification by plasma polymerization of ethanol and its application on oil-well cement, Appl. Surf. Sci. 409 (2017) 325–342.
[25] R. Nisticò, L. Lavagna, E.A. Boot, P. Ivanchenko, M. Lorusso, F. Bosia, N.M. Pugno, D. D'Angelo, M. Pavese, Improving rubber concrete strength and toughness by plasma-induced end-of-life tire rubber surface modification, Plasma Process. Polym. 18 (2021) 1–11.
[26] V. Mechtcherine, F.A. Silva, S. Muller, P. Jun, R.D.T. Filho, Coupled strain rate and temperature effects on the tensile behavior of strain-hardening cement-based composites (SHCC) with PVA fibers, Cement Concr. Res. 42 (11) (2012) 1417–1427.
[27] Q.H. Li, X. Gao, S.L. Xu, Multiple effects of nano-SiO2 and hybrid fibers on properties of high toughness fiber reinforced cementitious composites with high-volume fly ash, Cem. Concr. Compos. 72 (2016) 201–212.
[28] F.Y. Liu, K. Xu, W.Q. Ding, Y.F. Qiao, L.B. Wang, Microstructural characteristics and their impact on mechanical properties of steel-PVA fiber reinforced concrete, Cem. Concr. Compos. 123 (2021), 104196.
[29] W.J. Long, H.D. Li, L. Mei, W.W. Li, F. Xing, K.H. Khayat, Damping characteristics of PVA fiber-reinforced cementitious composite containing high-volume fly ash under frequency-temperature coupling effects, Cem. Concr. Compos. 118 (2021), 103911.
[30] J.Q. Wang, Q.L. Dai, R.Z. Si, S.C. Guo, Investigation of properties and performances of Polyvinyl Alcohol (PVA) fiber-reinforced rubber concrete, Construct. Build. Mater. 193 (2018) 631–642.
[31] Z.P. Chen, Y.H. Liang, Y.Z. Lin, J.M. Cai, Recycling of waste tire rubber as aggregate in impact-resistant engineered cementitious composites, Construct. Build. Mater. 359 (2022), 129477.
[32] A. Ai-Fakih, B.S. Mohammed, M.S. Liew, On rubberized engineered cementitious composites (R-ECC): a review of the constituent material, Case Stud. Constr. Mater. 14 (2021), e00536.
[33] L.L. Ma, B. Wang, L. Zeng, Y.F. Xiao, H. Zhang, Z. Li, Experimental investigation on the effect of rubber powder on mechanical properties of PVA fiber concrete, Adv. Civ. Eng. (2021) 1–12.
[34] S. Yeşilmen, Y. Al-Najjar, M.H. Balav, M. Şahmaran, G. Yıldırımc, M. Lachemi, Nano-modification to improve the ductility of cementitious composites, Cement Concr. Res. 76 (2015) 170–179.
[35] GB/T 2419, Test Method for Fluidity of Cement Mortar, Standards Press of China, China, 2005.
[36] GB/T 50080, Standard for Test Method of Performance on Ordinary Fresh Concrete, Standards Press of China, China, 2016.
[37] GB/T 17671, Method of Testing Cements-Determination of Strength, Standards Press of China, China, 1999.
[38] S. Muthusamy, S. Wang, D.D.L. Chung, Unprecedented vibration damping with high values of loss modulus and loss tangent, exhibited by cement–matrix graphite network composite, Carbon 48 (5) (2010) 1457–1464.
[39] J.P. Ou, T.J. Liu, J.L. Li, Dynamic and seismic property experiments of high damping concrete and its frame models, J. Wuhan Univ. Technol.-Materials Sci. Ed. 23 (2008) 1–6.
[40] J.F. Georgin, J.M. Reynouard, Modeling of structures subjected to impact: concrete behaviour under high strain rate, Cem. Concr. Compos. 25 (1) (2003) 131–143.
[41] H.D. Li, Q.M. Zhang, G.L. Feng, L. Mei, Y.C. Wang, W.J. Long, Multi-scale improved damping of high-volume fly ash cementitious composite: combined effects of polyvinyl alcohol fiber and graphene oxide, Construct. Build. Mater. 260 (2020), 119901.
[42] S. Rajaei, P. Shoaei, M. Shariati, F. Ameri, H.R. Musaeei, B. Behforouz, J. Brito, Rubberized alkali-activated slag mortar reinforced with polypropylene fibres for application in lightweight thermal insulating materials, Construct. Build. Mater. 270 (2021), 121430.
[43] D.V. Bompa, A.Y. Elghazouli, Creep properties of recycled tyre rubber concrete, Construct. Build. Mater. 209 (2019) 126–134.
[44] S.M.A. Qaidi, Y.Z. Dinkha, J.H. Haido, M.H. Ali, B.A. Tayeh, Engineering properties of sustainable green concrete incorporating eco-friendly aggregate of crumb rubber: a review, J. Clean. Prod. 324 (2021), 129251.
[45] L. Yan, C.H. Jenkins, R.L. Pendleton, Polyolefin fiber-reinforced concrete composites: Part I. Damping and frequency characteristics, Cement Concr. Res. 30 (3) (2000) 391–401.
[46] N. Swamy, G. Rigby, Dynamic properties of hardened paste, mortar and concrete, Mater. Struct. 4 (1) (1971) 13–40.
[47] D.D.L. Chung, Structural composite materials tailored for damping, J. Alloy Compos. 355 (1–2) (2003) 216–223.
[48] C. Liang, T. Liu, J. Xiao, D. Zou, Q. Yang, Effect of stress amplitude on the damping of recycled aggregate concrete, Materials 8 (8) (2015) 5298–5312.
[49] D.D.L. Chung, Interface-derived extraordinary viscous behavior of exfoliated graphite, Carbon 68 (2014) 646–652.
[50] Q. Zeng, K. Li, T. Fen-Chong, P. Dangla, Pore structure characterization of cement pastes blended with high-volume fly-ash, Cement Concr. Res. 42 (1) (2012) 194–204.
[51] C. Lin, L. Shuang, Y. Yan, Damping additives used in cement-matrix composites: a review, Compos. B Eng. 164 (2019) 26–36.
[52] G.A. Nadal, B.J.M. Gadea, G.F. Parres, S.E. Juliá, A.J.E. Crespo, A.J. Segura, Analysis behaviour of static and dynamic properties of Ethylene-Propylene-Diene-Methylene crumb rubber mortar, Construct. Build. Mater. 50 (2014) 671–682.
[53] R.N. Swamy, P.S. Mangat, Influence of fiber geometry on the properties of steel fiber reinforced concrete, Cement Concr. Res. 4 (3) (1974) 451–465.
[54] S. Lu, D.D.L. Chung, Viscoelastic behavior of silica fume in absence of binder, ACI Mater. J. 149 (2015) 1–10.
[55] P.H. Chen, D.D.L. Chung, Comparative evaluation of cement-matrix composites with distributed versus networked exfoliated graphite, Carbon 63 (2013) 446–453.
[56] M. Ali, R. Briet, N. Chouw, Dynamic response of mortar-free interlocking structures, Construct. Build. Mater. 42 (2013) 168–189.